

Block Copolymer Adsorption at the Polymer Melt/Substrate Interface: The Effect of Matrix Competition

Robert Oslanec[†] and Russell J. Composto*

Department of Materials Science & Engineering and Laboratory for Research on the Structure of Matter, The University of Pennsylvania, Philadelphia, Pennsylvania 19104-6272

Petr Vlcek

Institute of Macromolecular Chemistry, Academy of Sciences of the Czech Republic, Heyrovsky Square 2, 162 06 Prague 6, Czech Republic

Received July 30, 1999; Revised Manuscript Received January 3, 2000

ABSTRACT: Using low-energy forward recoil spectrometry (LE-FRES) and neutron reflectivity (NR), the interfacial excess, z^* , of an asymmetric poly(deuterated styrene-*block*-methyl methacrylate) (dPS-*b*-PMMA) at the polymer matrix/silicon oxide interface was found to decrease as the bromostyrene mole fraction, x , in a poly(styrene-*ran*-4-bromostyrene) (PBr_{*x*}S) matrix systematically increased. For matrix degrees of polymerization, $P = 480$ and 3846, z^* decreased by 15% and 33%, respectively, as x increased. Neglecting the matrix–substrate interaction energy, ϵ_M^s , self-consistent mean-field (SCMF) calculations predicted an increase in z^* with x , consistent with an increase in unfavorable matrix–dPS interactions, χ . By including a small attractive interaction ($\epsilon_M^s = -0.01k_B T$) between the matrix and substrate, the SCMF z^* decreased by ca. 50%, in qualitative agreement with experiments. Thus, as x increased (and therefore ϵ_M^s), matrix chain competition for silicon oxide counteracts the expected increased adsorption due to χ . Furthermore, the dPS volume fraction profile in PBr_{0.136}S had a lower z^* and was thinner than for the neutral matrix case.

Introduction

Polymer surface and interface properties underlie many applications including microelectronics, coatings, and paints. In many cases, adhesion between a polymer film and substrate is poor and must be improved by, for example, adding adhesion promoters to a formulation. Both end-functionalized homopolymers and block copolymers are attractive additives because they can be designed to anchor to the substrate while entangling with matrix chains. In addition to anchor strength, adhesion promotion will depend on the interpenetration between free ends of the attached chain and the matrix chains. This interfacial width is mainly governed by the degrees of polymerization of the additive and matrix (N and P , respectively) as well as segment–segment interactions. For block copolymer adsorption from a neutral matrix, we have shown that the interfacial excess, z^* , initially increases rapidly as P increases and then becomes constant for $P > 2N$, where N is the nonadsorbing block length.¹ Using a self-consistent mean-field model to interpret results, a crossover from a stretched to collapsed brush was attributed to the entropic repulsion of long matrix chains as P increased. In the present paper, block copolymer adsorption properties are studied as a function of matrix species. Specifically, the interfacial properties are manipulated by systematically increasing the unfavorable segment–segment interaction, χ , between the matrix and nonadsorbing block of the copolymer. Although matrix chains will be progressively expelled from the brush as χ increases, the interaction energy between matrix chains and the substrate will be shown to dominate the adsorption properties of the block copolymer.

Scaling laws² predict that polymer adsorption is relatively insensitive to the interactions between matrix chains and adsorbing polymers at low grafting densities but strongly dependent at high densities. In particular, unfavorable interactions will increase the net driving force for adsorption, resulting in a dense adsorbed layer and a sharp interface. On the other hand, a favorable matrix will decrease adsorption. In a favorable matrix, adsorbed chains are stretched and the matrix chains penetrate into the adsorbed layer. Correspondingly, the interface between the adsorbed layer and the matrix will be broad.

In this paper, the interaction energy between matrix chains and the substrate will influence adsorption. If attractive, the matrix chains will compete with the copolymer for adsorption sites. On the other hand, if this interaction is repulsive, the matrix chains are depleted from the interface, thus enhancing copolymer adsorption. To interpret results, we apply a self-consistent mean-field (SCMF) model that includes both the interaction energy between the adsorbing block and the substrate as well as that between the matrix and substrate. Experimentally, as the matrix species changes, the matrix–copolymer interactions and matrix–wall interactions will both change. *One great advantage of the SCMF model is that the matrix–wall interaction can be varied while holding other parameters fixed.* Using the SCMF as a guide, we will show that an increase in adsorption, due to unfavorable matrix–copolymer interactions, can be offset by a decrease in adsorption resulting from an attractive matrix–wall interaction (i.e., matrix competition).

Using neutron reflectivity (NR), Clarke and co-workers³ studied the adsorption of end-functionalized deuterated polystyrene (dPS–COOH) ($N = 710$ segments) at the polymer matrix/silicon oxide (SiO_{*x*}) interface for a variety of matrix species. Matrix polymers presenting

[†] Current address: BHP Institute of Steel Processing and Products, University of Wollongong, Wollongong, NSW 2522, Australia.

an unfavorable environment for dPS-COOH included poly(butadiene) (PB) ($P = 185$ and $10\,000$ segments) and poly(methyl methacrylate) (PMMA) ($P = 790$). The Flory-Huggins interaction parameters were $\chi_{\text{dPS-PB}} = 0.1$ and $\chi_{\text{dPS-PMMA}} = 0.037$, respectively. Polystyrene provided a neutral matrix where $\chi_{\text{dPS-PS}} \sim 0.0001$. Favorable matrices ($\chi < 0$) included poly(vinyl methyl ether) (PVME) ($P = 1710$) and a miscible blend (1:1) of PS ($P = 4815$) and poly(phenylene oxide) (PPO) ($P = 2620$). For $\chi < 0$, dPS chains were strongly stretched and the layer/matrix interface was broad, whereas for $\chi > 0$, the adsorbed layer was relatively thin and the layer/matrix interface sharp. In a limited test, the volume fraction profiles predicted from SCMF were found to be in agreement with NR results. Unfortunately, a quantitative comparison between systems was hindered by the matrix characteristics, including differences in P and polydispersity. Recently, Sferrazza and co-workers⁴ used NR to study the adsorption of end-grafted dPS as a function of the interaction parameter, $\chi_{\text{PVME/dPS}}$, between a PVME matrix and dPS. As temperature increased (i.e., $\chi_{\text{PVME/dPS}}$ increased), the PVME matrix chains were progressively expelled from the dPS brush. The influence of $\chi_{\text{PVME/dPS}}$ on brush thickness was in agreement with scaling predictions. Experiments in refs 3 and 4 demonstrate that end-functionalized homopolymer adsorption strongly depends on the matrix species. Diblock copolymer adsorption is relatively more difficult to understand because each block will interact differently with the matrix species.

Using forward recoil spectrometry (FRES), Green and Russell⁹ studied block copolymer adsorption to silicon oxide from a dissimilar polymer matrix species. The adsorbing species was a short symmetric block copolymer dPS-*b*-dPMMA having 262 total segments. Four polymer matrices were studied. Polystyrene ($P = 4810$ – $17\,310$) provided a neutral environment for the nonadsorbing dPS block and a repulsive one for the adsorbing dPMMA block. Using a PMMA matrix ($P = 5000$), the environments for the dPS and dPMMA blocks were reversed. Two other matrices, poly(vinyl chloride) (PVC) ($P = 1350$) and a (1:1) miscible blend of PS and PPO ($P = 540$), were also studied. For these four matrices, dPS-*b*-dPMMA adsorbed to silicon oxide only from the PS matrix. In some cases (e.g., PMMA matrix), copolymer adsorption was most likely prevented by the matrix competition for the substrate. A quantitative explanation was beyond the scope of this study because several segment-segment and segment-wall interactions were unknown.

The substrate surface is an important consideration when choosing an adhesion promoter. For example, adhesion can be tuned using an end-functionalized polymer, whose end group will react with the substrate. In recent studies,^{6,7} the interaction energy of a carboxylic acid functional group with SiO_x was found to be an order of magnitude stronger than that of butadiene segments.⁸ This observation is consistent with the relatively weak van der Waals interaction between butadiene and silicon oxide,⁹ compared to the chemical reaction between COOH and the surface.⁶

For block copolymer adsorption, the copolymer-substrate interaction can be tuned by simply varying the number of segments on the adsorbing block. Unfortunately, the interaction energy per segment is difficult to determine because it requires measuring the number of segments in contact with the substrate. Qualitatively,

Table 1. PBr_xS Matrix Characteristics

	P	range of x^a	$\chi_{\text{BM}}^{b,c}$
system I	480	0–0.168	1.7×10^{-4} – 3.5×10^{-3}
system II	3846	0–0.208	1.7×10^{-4} – 4.73×10^{-3}

^a Determined by elemental analysis by QTI, Inc.²¹ ^b Calculated from refs 13 and 14 for 160 °C. ^c The $\chi_{\text{BM}} = 1.7 \times 10^{-4}$ corresponds to dPS-PS interaction, where $x = 0$.

the PMMA block in dPS-*b*-PMMA was found to adsorb to silicon oxide and aluminum oxide, but not to gold.⁵ On the other hand, poly(isoprene) (PI) blocks were more strongly attracted to gold than to silicon oxide.¹⁰ Also, poly(2-vinylpyridine) (PVP) was strongly attracted to SiO_x .^{11,12} Clearly, a reliable database of segment-substrate interaction energies is needed before block copolymer adsorption properties can be predicted from first principles.

In this paper, we study the adsorption of an asymmetric dPS-*b*-PMMA block copolymer blended with a model matrix, namely poly(styrene-*ran*-bromostyrene) (PBr_xS). This system was chosen because the segment-segment interaction parameter, χ , between the nonadsorbing dPS block and the matrix polymer can be systematically tuned by increasing x , the mole fraction of bromostyrene. The unfavorable nature of the interaction between PS (dPS) and PBr_xS has been documented.^{13,14} Our group has taken advantage of the tunability of χ to control both surface segregation in miscible dPS:PBr_xS blends¹⁵ and interfacial segregation at the polymer/polymer interface between PS/dPBr_xS: PBr_xS, where dPBr_xS and PBr_xS are miscible with each other but not with PS.¹⁶ The PBr_xS matrix also allows one to vary x (i.e., χ) at constant P . Furthermore, PBr_xS is monodisperse. For these reasons, PBr_xS is a model polymer for investigating the effect of matrix species on dPS-*b*-PMMA adsorption. The main experimental finding in this paper is that the interfacial excess, z^* , of the dPS block decreases slightly as χ increases. By including a small attraction between the matrix and substrate, a modified SCMF model shows that matrix adsorption to the substrate offsets the expected increase in z^* as χ increases.

Experiment

Materials and Sample Preparation. In this study, the adsorbing polymer was an asymmetric poly(deuterated styrene-*block*-methyl methacrylate) block copolymer (dPS-*b*-PMMA) purchased from Polymer Source, Inc.¹⁷ The dPS-*b*-PMMA had a short MMA block (44 segments), which adsorbs to silicon oxide, and a long dPS block ($N = 933$), which extends into the matrix. Because the dPS-silicon oxide interaction is weak, dPS segments are readily displaced by MMA segments at the substrate.¹⁸ For the MMA block with a mole percent of 4.5%, the interaction energy with silicon oxide was $\epsilon_A^s \approx -8k_B T$ per block, which yields an effective interaction energy of $-0.18k_B T$ per segment.¹ Because only some of the MMA segments are in direct contact with the substrate, the true interaction energy per segment will be higher.

The matrix polymer was poly(styrene-*ran*-4-bromostyrene) (PBr_xS), a random copolymer prepared by bromination of polystyrene purchased from Pressure Chemical, Inc.¹⁹ The bromination procedure was described in ref 20. To study adsorption conditions at $P < N$ and $P > N$, PBr_xS with segment numbers of $P = 480$ and 3846 were chosen. The PBr_xS matrix characteristics including the range of x and χ_{BM} are given in Table 1. Systems containing the low- and high- P matrix polymers are denoted as systems I and II, respectively.

The silicon substrates were prepared by first removing the native oxide with a 7 vol % HF:water solution (3 min). The

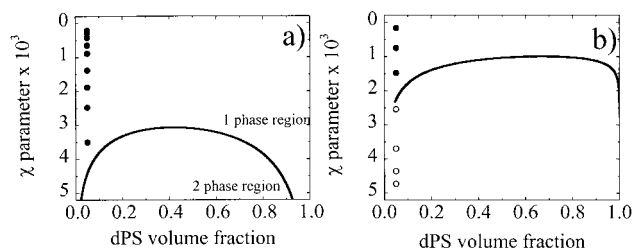


Figure 1. Phase diagram of dPS:PBr_xS blends where the dPS has 933 segments and PBr_xS has (a) 480 segments and (b) 3846 segments. The solid lines represent the boundary between the one-phase and two-phase regions. Solid and open circles represent samples in the one-phase and two-phase regions, respectively. Data correspond to 160 °C.

substrate was then placed in an ultraviolet ozone cleaner for 10 min to grow a ca. 20 Å thick silicon oxide film, as measured by ellipsometry.

Polymer films were prepared by spin-coating a toluene solution of dPS-*b*-PMMA and PBr_xS on a fresh substrate. Film thicknesses, as determined by ellipsometry, ranged from 2200 Å to about 2500 Å. The samples were annealed in a vacuum oven for 5 days at 160 °C. This annealing time was long enough to ensure equilibrium adsorption as determined from previous time-dependent studies.²² The volume fraction of dPS-*b*-PMMA in the as-cast films was $\phi_\infty = 0.05$.

Blend thermodynamics can play an important role in adsorption. For the low-*P* case (system I), the range of *x* was chosen such that an effective blend of the dPS block and PBr_xS would be miscible. Following,²³ the dPS:PBr_xS phase diagram is shown in Figure 1a. The critical χ parameter is $\chi_{c,I} = 3 \times 10^{-3}$. The solid circles in Figure 1a represent thin film samples for system I. For the high-*P* case (system II), the critical χ parameter decreases, $\chi_{c,II} = 1.2 \times 10^{-3}$. Therefore, over a similar range of *x* as system I, dPS:PBr_xS blends span the one-phase (solid circles) and two-phase (open circles) regions of the phase diagram, as shown in Figure 1b. We emphasize that the phase diagrams in Figure 1 serve only as a guide because they ignore the influence of the MMA block on blend thermodynamics.

Experimental Techniques. The interfacial excess of dPS was determined by low-energy, forward recoil spectrometry (LE-FRES) using a 2.0 MeV He⁺ ion beam at 15° incident and exit angles with respect to the polymer film and a 7.5 μm Mylar stopper foil. Under these conditions, the depth resolution was 450 Å at the surface and about 710 Å at 2200 Å beneath the surface. Conventional FRES²⁴ and LE-FRES²⁵ have been described elsewhere. For selected samples, the dPS volume fraction profiles were measured by neutron reflectivity at the Cold Neutron Research Facility at National Institute of Standards and Technology on the NG7 reflectometer. The principles of NR have been described elsewhere.²⁶ For consistency LE-FRES and NR measurements were performed on the same samples. The NR data sets were evaluated using the fitting procedure outlined in ref 15.

Self-Consistent Mean-Field Model. To help interpret experimental measurements, a SCMF model was used to calculate the volume fraction profiles of the dPS block at the PBr_xS/silicon oxide interface. The SCMF calculations followed the guidelines of Shull and Kramer²⁷ and were extended by us to study block copolymer adsorption at the polymer/solid interface. The SCMF input parameters are the segment numbers of both blocks and the matrix polymer, the bulk volume fraction of the copolymer, the Flory–Huggins segment–segment interaction parameters χ_{AB} , χ_{AM} , and χ_{BM} , and the interaction energies between the substrate and polymer segments, namely ϵ_A^s , ϵ_B^s , and ϵ_M^s . The index M denotes the matrix polymer, whereas A and B denote the PMMA and dPS blocks of the copolymer, respectively. Using the known dPS/PMMA interaction parameter,²⁸ the value of χ_{AB} was set to $\chi_{AB} = 0.0374$ at 160 °C. The χ parameter between dPS and PBr_xS, χ_{BM} , is a function of *x* and calculated from refs 13 and 14. The interaction between PMMA and PBr_xS, χ_{AM} , is not

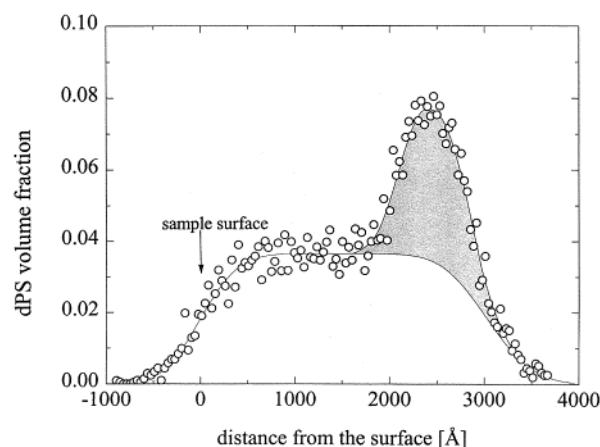


Figure 2. LE-FRES volume fraction profile of the dPS block in a dPS-*b*-PMMA:PBr_{0.15}S blend annealed at 160 °C for 5 days (open circles). The volume fraction of dPS in the as-cast sample is $\phi_\infty = 0.05$. The shaded area represents the dPS interfacial excess, z^* , and the arrow indicates the position of the sample surface.

known. However, large changes in χ_{AM} were found to change z^* by at most 2 Å.

The interaction energy of the MMA segment with the silicon oxide substrate, $\epsilon_A^s = -0.18k_B T$, was previously measured.¹ In the same studies, the interaction of dPS with silicon oxide was found to be negligible, $\epsilon_B^s = 0$. The interaction between PBr_xS and silicon oxide, ϵ_M^s , is not known, although it was observed^{29,30} that PBr_xS in a dPS:PBr_xS blend does not have a preference for silicon oxide. One goal of this paper is to investigate whether competition between PMMA and PBr_xS for adsorption sites will affect z^* . Using the SCMF model, we will perform this test by systematically varying ϵ_M^s , while holding all other parameters constant. For the interaction between PBr_xS and silicon oxide, the highly polar and electron-rich Br groups are likely to interact with Si–OH groups on the oxide surface via hydrogen bonding and induced dipole–dipole interactions. The SCF model in this paper does not account for the random copolymer nature of PBr_xS. To improve this model, the interactions between each segment type and the surface should be included.

Results

System I. Low Molecular Weight PBr_xS Matrix.

The adsorption of dPS-*b*-PMMA (*N* = 933) from a PBr_xS (*P* = 480) matrix is studied for bromostyrene mole fractions ranging from *x* = 0 to 0.168. Correspondingly, the dPS–PBr_xS segment–segment interaction parameter, χ_{BM} , increases from 1.7×10^{-4} to 3.5×10^{-3} . For this range of χ_{BM} , a dPS:PBr_xS blend is miscible for all concentrations as shown in Figure 1a. Using LE-FRES, we have measured the interfacial excess, z^* , of the dPS block at the PBr_xS/silicon oxide interface after vacuum annealing for 5 days at 160 °C. Figure 2 shows a representative dPS volume fraction profile in PBr_xS (*P* = 480) for the case *x* = 0.15. Within the resolution of LE-FRES, dPS-*b*-PMMA is uniformly distributed at the film surface and in the bulk. However, dPS-*b*-PMMA enrichment to the oxide surface is clearly observed as denoted by the shaded region (i.e., z^*) in Figure 2. The LE-FRES values of z^* are plotted as a function of χ_{BM} in Figure 3. As χ_{BM} varies by a factor of 20, z^* is relatively constant, showing only a small decrease from ca. 38 to 33 Å as χ_{BM} increases from 1.7×10^{-4} to 3.5×10^{-3} , respectively. Because this variation is within experimental error, the functional dependence of z^* on χ_{BM} could not be determined. Intuitively, these results

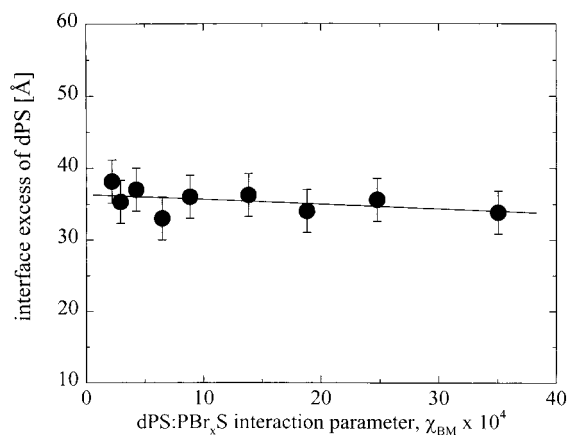


Figure 3. Interfacial excess of dPS determined by LE-FRES (solid circles) as a function of the matrix–dPS segment interaction energy for system I. The line is a guide to the eye. The error bars were obtained following ref 31.

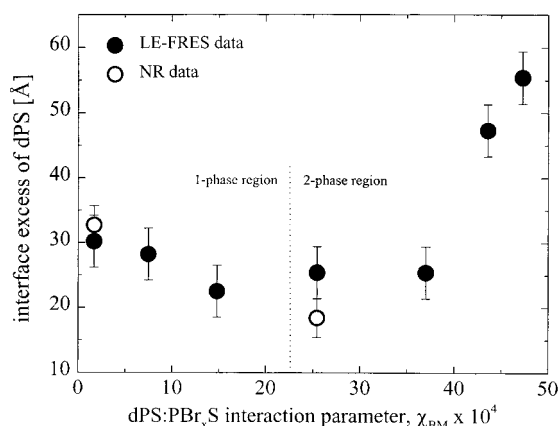


Figure 4. Interfacial excess of dPS determined by LE-FRES (solid circles) and NR (open circles) as a function of the matrix–dPS segment interaction energy for system II. The dotted line divides the one-phase and two-phase regions of the dPS:PBr_xS phase diagram shown in Figure 1b. The error bars were obtained following ref 31.

are particularly surprising because one expects the driving force for copolymer adsorption to increase as the interaction between the copolymer and matrix becomes less favorable. As discussed later, the expected increase in z^* due to χ_{AM} can be offset by competition from the matrix chains.

System II: High Molecular Weight PBr_xS Matrix.

The adsorption of dPS-*b*-PMMA ($N = 933$) from a PBr_xS ($P = 3846$) matrix is studied for x ranging from 0 to 0.208. Correspondingly, χ_{BM} increases from 1.7×10^{-4} to 4.7×10^{-3} . For system II, dPS:PBr_xS blends with x (χ_{BM}) greater than ca. 0.12 (2.25×10^{-3}) are expected to be immiscible as shown by the open circles in Figure 1b. For the same annealing conditions as system I, z^* is plotted as a function of χ_{BM} in Figure 4. Within experimental error, the z^* values determined by LE-FRES (solid circles) and NR (open circles) are in good agreement. For $\chi_{BM} < 2.25 \times 10^{-3}$ (i.e., one-phase), no surface segregation of dPS-*b*-PMMA was observed, whereas for $\chi_{BM} > 2.25 \times 10^{-3}$ (i.e., two-phase), surface enrichment was appreciable. This observation will be discussed in a future publication.²² In the one-phase region, z^* decreases from ca. 32 to 22 Å as χ_{BM} increases from 1.7×10^{-4} to 1.5×10^{-3} , respectively. Thus, by increasing the unfavorable interaction between copolymer and matrix polymer, copolymer adsorption de-

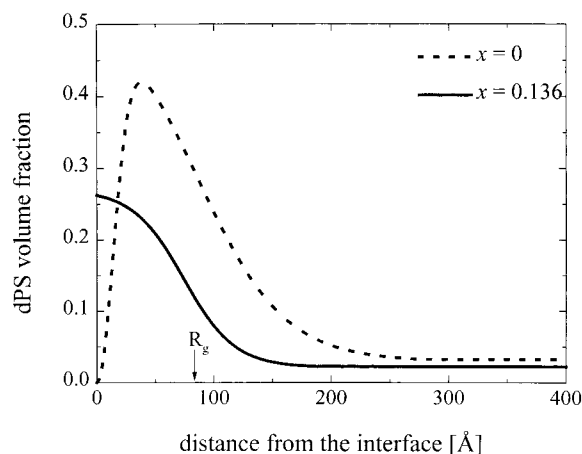


Figure 5. Volume fraction profiles of dPS at the interface between dPS-*b*-PMMA:PBr_xS and silicon oxide determined by NR for system II with $x = 0$ (dotted line) and $x = 0.136$ (solid line). The arrow indicates the radius of gyration of an unperturbed dPS block ($R_g \approx 85$ Å). The values of z^* are given in Figure 4.

creases by 30%, which is much stronger than observed in system I. However, for $\chi_{BM} > 2.25 \times 10^{-4}$, Figure 4 shows that z^* strongly increases by nearly a factor of 2 as χ_{BM} increases from 2.5×10^{-3} to 4.7×10^{-3} . In this regime, a quantitative analysis of z^* is greatly complicated by the two-phase nature of the film and will not be addressed in this paper.

Figure 5 shows the volume fraction profile of the dPS block measured by NR for PBr_xS matrices corresponding to $x = 0$ (dotted line) and $x = 0.136$ (solid line). The goodness of the fit is determined by minimizing the chi-square, χ^2 , between the measured and calculated reflectivities. The profiles in Figure 5 provide the minimum χ^2 , which range from 3 to 5. For the neutral PS matrix, the adsorbed layer is relatively thick and dense. The z^* is ca. 33 Å, in good agreement with LE-FRES measurements (see Figure 4). The dPS volume fraction reaches a maximum value of ca. 42% at a distance of 50 Å from the interface. The depletion layer between 0 and 50 Å is consistent with a thin adsorbed layer of the PMMA block. A depletion of dPS adjacent to the substrate also suggests that the interaction energy between dPS and silicon oxide, ϵ_{BS}^s , is negligible. As the matrix becomes unfavorable for the copolymer (solid line), the adsorbed layer collapses and its thickness becomes less than the dPS block radius of gyration, R_g , depicted by the arrow in Figure 5. Because the dPS volume fraction in the adsorbed layer is reduced, the z^* is only ca. 18 Å, in fair agreement with LE-FRES (see Figure 4). In contrast to the PS matrix, a depletion layer is no longer present, indicating that the dPS segments are driven to the substrate because of the unfavorable matrix environment.

Discussion

We have designed a thin film system containing a dPS-*b*-PMMA diblock having a long nonadsorbing dPS block and short adsorbing MMA block. An MMA mole fraction of 4% is chosen because this copolymer composition produces the highest grafting density.²² This adhesion promoter is blended with the majority component, PBr_xS, where x is the mole fraction of brominated styrene units. One reason for choosing this system is that the unfavorable segmental interaction energy between PBr_xS and dPS, denoted as χ_{BM} , is known to

increase as x increases (i.e., $\chi_{BM} \propto x^2$).^{13,14} Intuitively, one expects z^* to increase as χ_{BM} increases. In other words, one expects an increase in interfacial segregation as x increases. Indeed, our SCMF calculations show that the interfacial excess of the dPS block increases with increasing χ_{BM} if the other interactions are held fixed. Experimentally, z^* slightly decreases as χ_{BM} increases for the short matrix chains in system I (Figure 3) and clearly decreases for the long matrix chains in system II (Figure 4). The contradiction between the SCMF and experimental results can be reconciled by considering the other segment–segment and segment–wall interactions that depend on x .

Because the segment–segment interaction parameter, χ_{AM} , between PMMA and PBr_xS is unknown, we have investigated the effect of χ_{AM} on z^* by varying χ_{AM} over almost 2 orders of magnitude, from favorable to unfavorable, in SCMF calculations. As χ_{AM} becomes more favorable, z^* decreases because it is more favorable for the PMMA block to stay in the bulk than to adsorb at the interface. On the other hand, increasing the unfavorable interaction between PMMA and PBr_xS acts to increase z^* . Nevertheless, for both cases, z^* changes by less than 2 Å or only 7% of the experimental z^* . Therefore, we can conclude that the PMMA–PBr_xS interaction does not significantly influence dPS-*b*-PMMA adsorption at the PBr_xS/silicon oxide interface.

The interaction energy between the PBr_xS segments and silicon oxide substrate, ϵ_M^s , also depends on x . If $\epsilon_M^s < 0$, PBr_xS segments will be attracted to the oxide and possibly compete with dPS-*b*-PMMA for surface sites, resulting in a lower value of z^* . To test this hypothesis, SCMF calculations were performed as ϵ_M^s was systematically varied from $-0.10k_B T$ (attractive) to $+0.01k_B T$ (repulsive) while the other substrate interaction energies were held constant at $\epsilon_A^s = -0.18k_B T$ and $\epsilon_B^s = 0$.¹ The segment–segment interaction parameters were set to $\chi_{AB} = 0.0374$,²⁸ $\chi_{AM} = 0.0284$, and $\chi_{BM} = 5 \times 10^{-4}$. These χ parameters correspond to the PBr_xS matrix with $x = 0.03$. Using these χ parameters, SCMF calculations were performed for systems I and II. Because the results are qualitatively the same, only system I calculations are presented.

Figure 6 shows that z^* strongly increases as the matrix–substrate interaction energy becomes less favorable. Assuming an attractive interaction, z^* decreases from ca. 36 to ca. 5 Å as ϵ_M^s varies from 0 (a neutral substrate) to $-0.04k_B T$ (an attractive substrate). Recall that z^* was found to decrease by about 15% and 33% in systems I and II, respectively. For comparison, for the case $\epsilon_M^s = -0.01k_B T$, z^* decreases by about 50% relative to the neutral substrate. Note that this value of ϵ_M^s is almost 20 times weaker than the MMA–substrate interaction energy. Because the matrix interaction is amplified by P , a small segmental attraction for the substrate can dramatically reduce dPS-*b*-PMMA adsorption. This interpretation is consistent with the larger decrease in z^* observed for system II (Figure 4) which has the larger P . To provide further insight, the interfacial segregation of PBr_xS at the interface between dPS:PBr_xS and silicon oxide was modeled using SCMF. Using the previously mentioned interaction parameters, z^* was found to be quite small, only ca. 1 and 3.5 Å for $P = 480$ and 3846, respectively. This result is consistent with experimental studies, which were unable to detect segregation at the dPS:PBr_xS/silicon oxide interface.^{29,30}

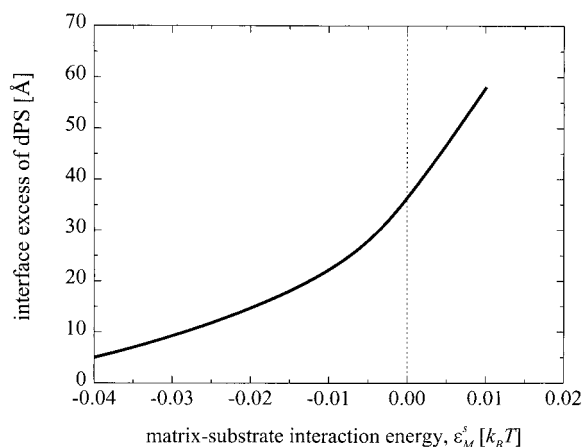


Figure 6. Interfacial excess of dPS calculated by the SCMF model (solid line) as a function of the matrix–substrate interaction energy, ϵ_M^s . The vertical dashed line at $\epsilon_M^s = 0$ denotes the crossover between favorable ($\epsilon_M^s < 0$) and unfavorable ($\epsilon_M^s > 0$) interactions between the matrix and substrate. As a reference, $\epsilon_M^s = -0.01k_B T$ is an order of magnitude weaker than ϵ_A^s , the MMA–substrate interaction.

Thus, in the dPS-*b*-PMMA:PBr_xS system, z^* decreases as x increases because of competition between the long PBr_xS chains and the short MMA blocks for surface sites.

The dPS volume fraction profiles in Figure 5 are in qualitative agreement with the profiles predicted by the SCMF model. For the PS matrix case ($x = 0$), the SCMF profile captures the shape and thickness of the experimental profile using the parameters given in this paper. Although the SCMF profile shows a slightly smaller depletion layer than the experimental profile, a quantitative comparison was not attempted because both the NR simulation and SCMF profiles are insensitive to small changes in concentration near the interface ($z = 0$ Å). A more comprehensive study is needed to address this issue. Nevertheless, the SCMF profile is strongly influenced by the matrix species. As x increases, the depletion layer decreases and eventually disappears as shown in Figure 5 for $x = 0.136$. Concurrently, the dPS interfacial excess decreases. As the interaction energy between the dPS block and matrix increases, the dPS layer thickness decreases to reduce unfavorable interactions. However, at a fixed dPS block–matrix interaction, the thickness remains constant as the matrix–substrate interaction becomes more favorable. We emphasize that one cannot perform this test experimentally because a change in matrix species will affect both the matrix–substrate and matrix–dPS interactions.

In summary, these SCMF calculations demonstrate that modeling of block copolymer adsorption must consider all possible segment–segment and segment–substrate interactions. Upon systematically increasing the unfavorable copolymer–matrix interactions, the expected increase in z^* was found to be offset by matrix competition for the substrate. By decoupling the influence of the matrix–dPS and matrix–substrate interactions, the SCMF model has proven to be a powerful tool for interpreting experimental results.

Conclusion

In this paper, the adsorption of dPS-*b*-PMMA to the interface between PBr_xS and silicon oxide is studied as a function of the degree of bromination, x , and P , the

matrix segment number. In system I, P is $1/2N$, the dPS segment number; in system II, P is ca. $8N$. The former system results in a wet brush whereas the latter corresponds to a relatively dry brush. As x increases, the unfavorable dPS–PBr₃S interactions increase, and intuitively the interfacial excess, z^* , of the dPS is expected to increase. However, for systems I and II, z^* decreases as x increases. To interpret these results, a SCMF model is developed that incorporates all segment–segment and segment–wall interactions. The SCMF calculations show that neither χ_{AM} nor χ_{BM} can account for the observations revealed by LE-FRES and NR. On the other hand, a small attractive interaction energy between the matrix and substrate, $\epsilon_M^S = -0.01k_B T$, results in a significant reduction of z^* relative to a neutral substrate. Thus, competitive adsorption of matrix chains is the likely reason for the lower than expected dPS-*b*-PMMA adsorption.

Acknowledgment. This research was supported by the National Science Foundation, Division of Materials Science, under Grants DMR99-74366 and DMR96-32598. The ion scattering experiments and SCMF calculations made use of the MRSEC Shared Experimental Facilities supported by NSF under Grant DMR96-32598. We thank Dr. Sushil Satija for assistance with reflectivity experiments at the NIST Center for Neutron Research (NCNR).

References and Notes

- (1) Oslanec, R.; Vlcek, P.; Hamilton, W. A.; Composto, R. J. *Phys. Rev. E* **1997**, *56*, 2383.
- (2) Aubouy, M.; Raphaël, E. *J. Phys. II* **1993**, *3*, 443.
- (3) Clarke, C. J.; Jones, R. A. L.; Edwards, J. L.; Shull, K. R.; Penfold, J. *Macromolecules* **1995**, *28*, 2042.
- (4) Sferrazza, M.; Jones, R. A. L.; Bucknall, D. G. *Phys. Rev. E* **1999**, *59*, 4434.
- (5) Green, P. F.; Russell, T. P. *Macromolecules* **1992**, *25*, 783.
- (6) Zhao, X.; Zhao, W.; Zheng, X.; Rafailovich, M. H.; Sokolov, J.; Schwarz, S. A.; Pudensi, M. A. A.; Russell, T. P.; Kumar, S. K.; Fetters, L. J. *Phys. Rev. Lett.* **1992**, *69*, 776.
- (7) Clarke, C. J.; Jones, R. A. L.; Edwards, J. L.; Clough, A. S.; Penfold, J. *Polymer* **1994**, *35*, 4065.
- (8) Jones, R. A. L.; Norton, L. J.; Shull, K. R.; Kramer, E. J.; Felcher, G. P.; Karim, A.; Fetters, L. J. *Macromolecules* **1992**, *25*, 2359.
- (9) Ahagon, A.; Gent, A. N. *J. Polym. Sci., Polym. Phys. Ed.* **1975**, *13*, 1285.
- (10) Budkowski, A.; Klein, J.; Fetters, L. J. *Macromolecules* **1995**, *28*, 8571.
- (11) Calistri-Yeh, M. Ph.D. Thesis, Cornell University, Ithaca, NY, 1995.
- (12) Liu, Y.; Schwarz, S. A.; Zhao, W.; Quinn, J.; Sokolov, L.; Rafailovich, M. H.; Iyengar, D.; Kramer, E. J.; Dozier, W.; Fetters, L. J.; Dickman, R. *Europhys. Lett.* **1995**, *32*, 211.
- (13) Strobl, G. R.; Bendler, J. T.; Kambour, R. P.; Shultz, A. R. *Macromolecules* **1986**, *19*, 2683. Strobl, G. R.; Urban, G. *Colloid Polym. Sci.* **1988**, *266*, 398.
- (14) Bruder, F.; Brenn, R. *Macromolecules* **1991**, *24*, 5552.
- (15) Genzer, J.; Faldi, A.; Oslanec, R.; Composto, R. J. *Macromolecules* **1996**, *29*, 5438.
- (16) Genzer, J.; Composto, R. J. *Macromolecules* **1998**, *31*, 870.
- (17) Polymer Source, Inc., Dorval, Canada.
- (18) Kobayashi, K.; Sugimoto, S.; Yajima, H.; Araki, K.; Imamura, Y.; Endo, R. *Bull. Chem. Soc. Jpn.* **1990**, *63*, 2018.
- (19) Pressure Chemical, Pittsburgh, PA.
- (20) Kambour, R. P.; Bendler, J. T.; Bopp, R. C. *Macromolecules* **1983**, *16*, 753.
- (21) Quantitative Technologies, Inc., Whitehouse, NJ. The reported accuracy of the analysis was $\pm 0.5\%$ of the bromine content.
- (22) Oslanec, R. Ph.D. Thesis, University of Pennsylvania, Philadelphia, PA, 1997.
- (23) de Gennes, P. G. *Scaling Concepts in Polymer Physics*; Cornell University Press: Ithaca, NY, 1979.
- (24) Mills, P. J.; Green, P. F.; Palmström, C. J.; Mayer, J. W.; Kramer, E. J. *Appl. Phys. Lett.* **1984**, *45*, 957.
- (25) Genzer, J.; Rothman, J. B.; Composto, R. J. *Nucl. Instrum. Methods* **1994**, *B86*, 345.
- (26) Russell, T. P. *Mater. Sci. Rep.* **1990**, *5*, 171.
- (27) Shull, K. R.; Kramer, E. J. *Macromolecules* **1990**, *23*, 4769. Shull, K. R. *J. Chem. Phys.* **1991**, *94*, 5723.
- (28) Russell, T. P.; Hjelm, Jr., R. P.; Seeger, P. A. *Macromolecules* **1990**, *23*, 890. Russell, T. P. *Macromolecules* **1993**, *26*, 5819.
- (29) Bruder, F.; Brenn, R. *Phys. Rev. Lett.* **1992**, *69*, 624.
- (30) Genzer, J. Private communication.
- (31) The results were obtained by minimizing the χ^2 between the experimental and simulated data. To estimate error bars, we varied the corresponding parameter such that χ^2 increased by a factor of about 2.

MA991269+